

## The Elastic Scattering and Capture of Protons by Oxygen\*

R. A. LAUBENSTEIN,† M. J. W. LAUBENSTEIN,† L. J. KOESTER,‡ AND R. C. MOBLEY  
*University of Wisconsin, Madison, Wisconsin*

(Received June 18, 1951)

The yield of elastically scattered protons from oxygen was measured with a magnetic analyzer which detected protons scattered through laboratory angles of  $159^\circ$  to  $169^\circ$ . Using protons accelerated by an electrostatic generator, the proton energy range from 0.6 to 4.5 Mev was covered in 4.4-keV or smaller steps. Two sharp resonances were observed, one at an incident proton energy of 2.66 Mev with a width of 19.9 keV, and the second at 3.47 Mev with an observed width less than 3.5 keV. Near 4.0 Mev a broad maximum in the cross section was obtained, and a broad resonance appears to give another maximum slightly above 4.5 Mev. The resonance at 2.66 Mev appeared as a nearly symmetrical dip in the scattering cross section.

The capture cross section of oxygen for protons was measured for incident proton energies from 1.4 to 4.1 Mev by counting the positrons from the decay of  $F^{17}$  built up under the bombardment of oxide targets. Up to a narrow resonance at 3.47 Mev, the capture cross section was observed to increase almost linearly with energy. Above 3.75 Mev, the cross section was found to increase more rapidly to a maximum near 3.99 Mev.

On the basis of the scattering and capture data, energy levels have been assigned to  $F^{17}$  at 3.11, 3.88, 4.36, and 4.73 Mev, although the positions of the latter two levels are not clearly defined by the data.

### I. INTRODUCTION

A STUDY of the interaction of protons with  $O^{16}$  yields information about the energy levels of the compound nucleus,  $F^{17}$ . Although this nucleus has been investigated previously, little information is available on the location of the energy levels or their character. Because oxygen is so often a contaminant in target materials, a knowledge of the reactions of protons with oxygen is also important in connection with other experiments. Certain nuclear properties of  $O^{16}$  and of the interaction of protons with  $O^{16}$  make this reaction not only interesting, but also well suited to a comparison of theory and experiment. A discussion of such a comparison is given in the paper which follows.<sup>1</sup>

In the range of incident proton energies from 0.6 to 4.5 Mev which this experiment covers, previous investigations of the interaction of protons have been comparatively few. Heitler, May, and Powell<sup>2</sup> measured the

angular distribution of 4.2-Mev protons elastically scattered from oxygen. Using 4.5-Mev protons, Rhoderick<sup>3</sup> looked for protons inelastically scattered from oxygen but did not observe any. The capture of protons by oxygen has been investigated most extensively by DuBridge, Barnes, Buck, and Strain,<sup>4,5</sup> who used the stacked foil technique to obtain an excitation curve which indicates a resonance near 3.5 Mev and a rapidly increasing yield near 3.9 Mev.

### II. ELASTIC SCATTERING OF PROTONS BY OXYGEN

#### Apparatus and Procedure

The yield of elastically scattered protons from oxygen was measured as a function of incident proton energy by using a magnetic analyzer to separate protons scattered by oxygen from protons scattered by other elements in the target. A detailed description of the design and construction of the analyzer and associated equipment is given elsewhere.<sup>6-8</sup> Figure 1 shows a horizontal cross section of the analyzer and the proton paths. Protons scattered by the target through laboratory angles of  $159^\circ$  to  $169^\circ$  enter the analyzer where only those protons with the correct momentum are allowed to pass between the exit slits and enter the proportional counter. Separating the counter from the evacuated region of the analyzer was a nickel foil 0.00005 inch thick. By means of a magnetic balance-type fluxmeter<sup>9,10</sup> the magnetic field was set or its value measured to an accuracy of about 0.15 percent. The Wisconsin electro-

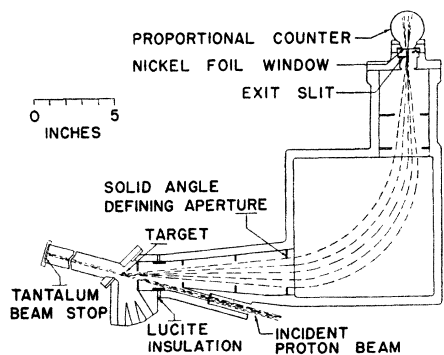


FIG. 1. Horizontal cross section of the magnetic analyzer, showing the proton paths.

\* Supported by the Wisconsin Alumni Research Foundation and the AEC.

† Now at North American Aviation, Inc., Downey, California.

‡ AEC Predoctoral Fellow.

<sup>1</sup> R. A. Laubenstein and M. J. W. Laubenstein, *Phys. Rev.* **84**, 18 (1951).

<sup>2</sup> Heitler, May, and Powell, *Proc. Roy. Soc. (London)* **190**, 180 (1947).

<sup>3</sup> E. H. Rhoderick, *Proc. Roy. Soc. (London)* **201**, 348 (1950).

<sup>4</sup> DuBridge, Barnes, and Buck, *Phys. Rev.* **51**, 995 (1937).

<sup>5</sup> DuBridge, Barnes, Buck, and Strain, *Phys. Rev.* **53**, 447 (1938).

<sup>6</sup> J. E. Faulkner, thesis, University of Wisconsin (1950), unpublished.

<sup>7</sup> G. M. B. Bouricius, thesis, University of Wisconsin (1950), unpublished.

<sup>8</sup> Shoemaker, Faulkner, Bouricius, Kaufmann, and Mooring, to be published.

<sup>9</sup> Buechner, Strait, Sperduto, and Malm, *Phys. Rev.* **76**, 1543 (1949).

<sup>10</sup> G. Goldhaber, unpublished.

static generator provided a collimated proton beam with a well-defined energy spread. For this experiment, a beam current of about  $0.4 \mu\text{a}$  was incident on a target area 2 mm square.

In order to avoid other elements which would give reactions under proton bombardment, only oxides of heavy elements were used as targets. The entire yield curve (shown in Fig. 3) was taken with a target of barium oxide on a backing of 1000A nickel foil. A description of the mounting and preparation of the foils is given by Bashkin and Goldhaber.<sup>11</sup> Barium oxide was deposited on these foils by evaporating a thin film of barium and then admitting dry air to the evaporator in order to allow the oxide to form.

Figure 2, a typical momentum analysis, shows that for an exit slit width of 10 mm, which was used for this experiment, the protons scattered from oxygen and from carbon can be almost completely resolved by the analyzer. Certain characteristics of the analyzer, calculated in terms of  $H\rho$ , are included in Fig. 2 and indicate why the particular shape of the oxygen "peak" is obtained. There is a range of magnetic field values over which all of the protons scattered by oxygen will pass between the exit slits of the analyzer and be detected.

Momentum analyses of the protons scattered from the target were taken at frequent intervals and served to calibrate the fluxmeter and determine the background correction. All of the momentum analyses showed a background of protons counted at magnetic field settings for which no protons should enter the counter. Some of this background was observed with no target in place and was caused by protons scattered within the analyzer so that they entered the counter. Approximately an equal background resulted from protons scattered first by nickel, barium, or other heavy elements in the target and rescattered in the analyzer slit system so that they entered the counter at relatively low magnetic field settings. Over the energy range for which the oxygen and nickel peaks were well separated, the total background was obtained by extrapolating the yield between these peaks into the oxygen peak. For the target of barium oxide on 1000A nickel with which most of the data were taken, the background was about 5 percent of the yield of protons scattered from oxygen, except at energies below 1 Mev.

As the incident proton energy was decreased, several effects contributed to an increasing uncertainty in the measurement of the relative scattering cross section. At low energies the nickel peak spread out because of increasing target thickness and began to overlap the oxygen peak. In order to overcome the uncertainty in yield caused by this overlap, data taken below 1 Mev with the target used for the entire curve were normalized to data obtained with a target of barium oxide on a 500A nickel foil and a target of barium oxide on

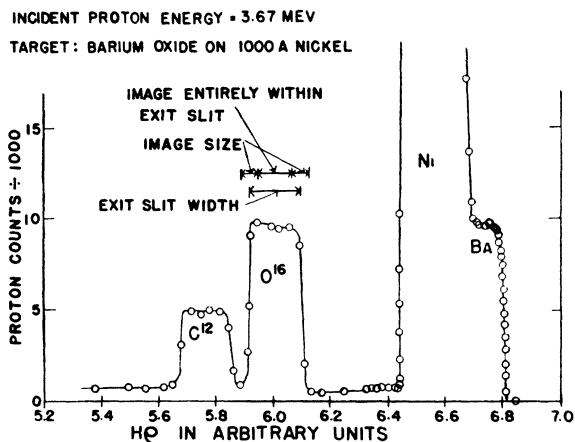


FIG. 2. Momentum analysis of protons scattered from a target of BaO on 1000A nickel foil.

diamond. Use of these targets also eliminated the necessity of corrections to the low energy yield because of oxygen which was found to occur on the back surface of the nickel foil. This oxide layer is normally found on nickel, but may have been enhanced here by the chemicals used in the preparation of the foils. At high energies, protons scattered by oxygen on both sides of the nickel pass through the analyzer, but at low energies this is no longer true, and the 5 percent yield obtained from oxygen on the back side will not be present in the main oxygen peak. Increased thickness of the oxygen-containing layer on the target caused an increase in the size of the image formed by protons scattered from oxygen, and this image took up a larger fraction of the exit slit width giving a narrower and more rounded peak at low energies. Thus, below 1 Mev, it was necessary to change the magnetic field every time that the energy of the incident protons was changed. The results were a larger scattering of the data points and more uncertainty in the low energy region of the curve.

## Results

The yield curve obtained for the elastic scattering of protons by oxygen is shown in Fig. 3. Data shown on this curve were all taken with an incident proton energy spread of 0.18 percent at half-maximum intensity, except near the 3.47-Mev resonance, where data are shown for 0.06 percent energy spread. Above 1.35 Mev, data points were obtained no more than 4.4 kev apart, and below this energy no more than 2.9 kev apart. Each point represents about 12 microcoulombs of protons striking the target. Accurate measurement of this proton charge was made with a current integrator designed by Bouricius and Shoemaker.<sup>12</sup>

A differential cross section of  $3/4\pi$  barn per steradian on the yield curve corresponds to about 7400 recorded proton counts above background. The statistical uncer-

<sup>11</sup> S. Bashkin and G. Goldhaber, Rev. Sci. Instr. **22**, 112 (1951).

<sup>12</sup> G. M. B. Bouricius and F. C. Shoemaker, Rev. Sci. Instr. **22**, 183 (1951).

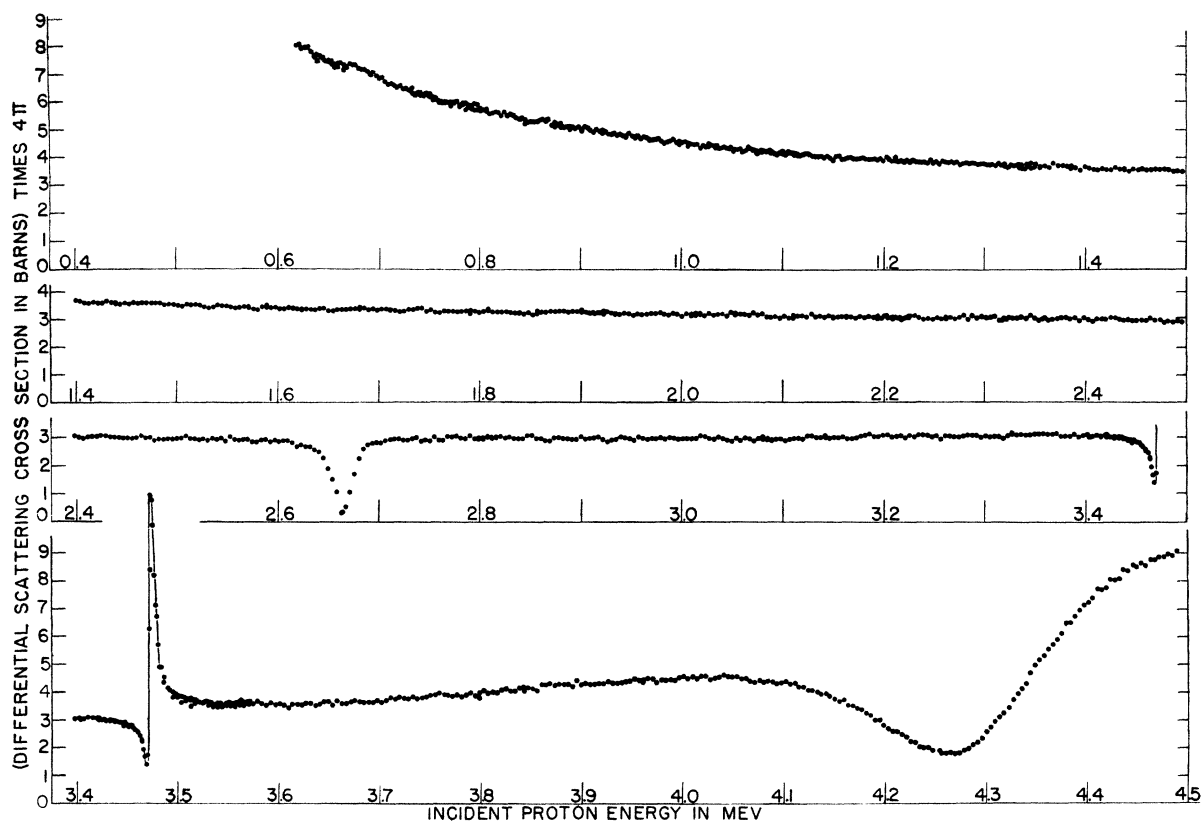


FIG. 3. Yield of protons elastically scattered from oxygen through laboratory angles  $159^{\circ}$ - $169^{\circ}$ .

tainties are everywhere smaller than the circles which represent the data points. Above 1.1 Mev, the relative cross sections should be accurate to  $\pm 4$  percent except near the 2.66-Mev and 3.47-Mev resonances, while below 1.1 Mev, where additional uncertainties were introduced in the background corrections, the relative values may be accurate to only  $\pm 15$  percent. A large error may be expected in the absolute value of the cross sections indicated by the ordinate scale. Many of the small variations in the yield curve occur at energies where the magnetic field was changed and are caused by the sloping top of the oxygen peak. None of these variations, including the largest at 0.66 Mev, are real. The contributions of the  $O^{17}$  and  $O^{18}$  isotopes should not be larger than the statistical uncertainty.

In order to plot the shape of the resonance at 2.66 Mev as accurately as possible, thin targets (0.6-0.25 kev) and a proton beam energy resolution of 0.04 percent and 0.02 percent at half-maximum intensity were used. Because the thickness of the nickel was not small compared with the width of the resonance, the oxygen on the back side of the foil or in the foil, a large percentage of the total for thin targets, made large corrections necessary. To avoid these corrections, the target with the diamond backing was employed. A plot of the best results obtained for this 2.66-Mev resonance, which appears as an almost symmetrical dip in the

cross section, is shown together with a theoretical fit in the paper which follows.<sup>1</sup> A ratio of maximum to minimum cross section of 11.5 was obtained, and the fit of the resonance gives an observed width,  $\Gamma$ , of 19.9 kev. It must be emphasized that the background at the minimum of the resonance was a large part of the total yield and that the value given for the minimum may be in error by as much as a factor of two.

The resonance at 3.47 Mev was sufficiently narrow so that its shape could not be accurately determined with the smallest beam energy spread and the thinnest targets available. A cross section at the maximum of  $16/4\pi$  barns per steradian relative to the scale shown on Fig. 3 was obtained, but the narrowness of the peak of the resonance makes this value uncertain. The width of the resonance is less than 3.5 kev.

Two broad resonances are indicated in the high energy region of the curve, and it appears as if there is interference between these levels, thus making an interpretation of this part of the curve difficult. The gradual increase of the scattering cross section from 3.6 to 4.0 Mev must be caused by a resonance, although the location of the resonance cannot be obtained from a visual inspection of the scattering yield curve. A more detailed analysis of the data indicates that the minimum near 4.27 Mev and the maximum near 4.5 Mev may be caused by another resonance at an incident proton

energy of about 4.39 Mev and with an observed width,  $\Gamma_{\text{lab}}$ , of about 0.24 Mev.

In the low energy region the scattering cross section does not decrease with increasing energy as fast as for Rutherford-type scattering, and by comparison the experimental cross section is relatively flat. Some experimental data were obtained on the scattering of protons by oxygen in the energy range from 450 to 600 kev using a scintillation counter. Changes in the efficiency of the counter with energy and a large background made an accurate normalization of these data impossible. The data did indicate that there were no rapid changes in the cross section between 450 and 600 kev, and hence no resonances occur in that energy range.

Attempts to measure the absolute cross section were made. In the various momentum analyses taken at different energies the yield of elastically scattered protons from barium was obtained, and the scattering cross section for barium was found to vary as the reciprocal of the square of the energy. Therefore, the scattering from barium was assumed to be of the Rutherford type for which the cross section can be calculated. Assuming that the compound in the target was BaO, then the cross section for oxygen was the ratio of the yield of protons from oxygen to the yield of protons from barium times the Rutherford cross section of barium. The best experimental value for the cross section is  $3.1/4\pi$  barns per steradian in the laboratory system at an incident proton energy of 2.2 Mev. This value was used in drawing the ordinate scale of Fig. 3. In the momentum analyses the dip between the oxygen and carbon peaks was sufficiently low to conclude that nitrogen was not detectable in the target and thus that barium nitride was not formed. Other possible compounds of barium which might have formed instead of the oxide, i.e., barium hydroxide or barium carbonate, give more than one oxygen atom for each barium atom and would result in a lower calculated cross section. During storage of the barium oxide targets in a desiccator, some of the barium oxide may have been converted to these other barium compounds. If all of the oxide were converted to the carbonate, the cross section given above would be too high by a factor of 3. However, the upper limit to the differential scattering cross section given here is an aid in an analysis of the data, and such an analysis indicates that the cross sections given in Fig. 3 are too large by 22 percent.

### III. CAPTURE OF PROTONS BY OXYGEN

The capture of protons by  $\text{O}^{16}$  produces  $\text{F}^{17}$  with the emission of one or more gamma-rays to carry away the excess energy. Since the  $Q$  value of 0.61 Mev is lower than for any other ( $p,\gamma$ ) reaction and since the capture cross section is small, the capture gamma-rays are difficult to detect above the background radiation produced by the electrostatic generator and by the annihilation of the positrons emitted by  $\text{F}^{17}$ . However, the

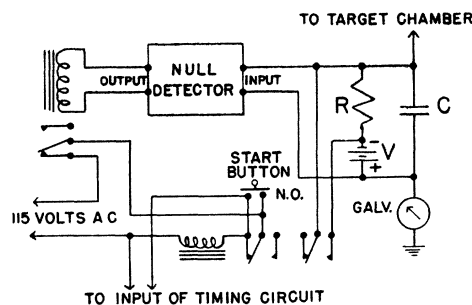


FIG. 4. Electric circuit used to compensate for fluctuating beam current and measure the activity built up in the target during bombardment.

detection of these positrons provides a sensitive method of measuring the capture of protons by  $\text{O}^{16}$ .

### Apparatus and Procedure

An investigation of the capture cross section from 1.1 to 4.1 Mev was made by bombarding oxide targets with protons from the electrostatic generator and taking the resulting  $\text{F}^{17}$  activity as a measure of the capture cross section. In order to build up a reasonable activity in the target, it was desirable to bombard the targets for a time comparable to the half-life of  $\text{F}^{17}$ , which was measured and found to be  $66.3 \pm 1$  seconds. If the beam current is not constant, the activity in the target at the end of bombardment will be a function of the variation of the beam current as well as the average current and the bombardment time.

Figure 4 shows an electric circuit similar to one described by Snowdon<sup>13</sup> which was used to measure the activity built up in the target. Except for the resistance  $R$ , this circuit is that of the current integrator of Bouricius and Shoemaker,<sup>12</sup> which has a null detector as its essential feature. The operation of the circuit, which will hereafter be called the normalization circuit, may be described as follows: Normally, the condenser  $C$  is charged to a voltage  $V$  by the battery connected across it through a relay. During bombardment the proton current which strikes the target is allowed to discharge the condenser. When the null detector indicates that the condenser voltage is zero, the beam is shut off. If the beam current should be interrupted during bombardment, the condenser will recharge through the resistance  $R$  at the same rate at which the radioactive product decays, because the time constant,  $RC$ , is set equal to the mean life of the radioactivity.

Table I compares the differential equation and its solution for the electric circuit with that of the build-up of radioactivity in the target. The notation is:  $I$  = proton current as a function of time,  $E_C$  = potential of the upper plate of condenser  $C$ ,  $V$  = battery voltage,  $\lambda$  = decay constant of the radioactive product,  $N$  = number of radioactive atoms in the target at time  $t$ ,  $t$  = time measured from the start of bombardment, and  $kI$  = rate

<sup>13</sup> S. C. Snowdon, Phys. Rev. 78, 299 (1950).

TABLE I. Comparison of electric circuit with build-up of radioactivity in the target.

	Electric circuit	Radioactive product
Differential equation	$\frac{d(V+E_c)}{dT} = \frac{(V+E_c)}{RC} + \frac{I}{C}$	$\frac{dN}{dt} = -\lambda N + kI$
Boundary condition	$(V+E_c) = 0$ at $t=0$	$N = 0$ at $t=0$
Solution	$(V+E_c) = \frac{1}{C} e^{-t/RC} \int_0^t e^{t/RC} I dt$	$N = k e^{-\lambda t} \int_0^t e^{\lambda t} I dt$

of formation of the radioactive atoms, where  $k$  is a constant depending on the cross section for the reaction and the target thickness.

Although the quantity  $E_c$  is actually measured by the null detector, the quantity  $(V+E_c)$  will be used as a variable to show the similarity in equations.

By putting  $RC = 1/\lambda$ , the two equations in the last row of Table I will give

$$(V+E_c) = N/kC. \quad (1)$$

At the end of bombardment  $E_c = 0$ , and Eq. 1 becomes

$$N = kCV. \quad (2)$$

Substituting for  $C$  gives

$$N = kV/\lambda R. \quad (3)$$

Equation 3 can be compared with the case where the beam current is constant and

$$N = (k/\lambda)I(1 - e^{-\lambda t}).$$

If the electric circuit is used, the activity in the target at the end of bombardment is equal to the activity obtained after infinite bombardment with a current  $V/R$ . Thus, the constants of the circuit must be adjusted so that  $V/R$  is less than the beam current available; and for a given beam current, the ratio  $V/R$  will determine the length of bombardment. In this experiment the radioactive product has a half-life of about 66 seconds, and the approximate values of the constants used are:  $C = 16 \mu\text{f}$ ,  $V = 6$  volts,  $R = 6$  megohms,  $V/R = 1 \mu\text{a}$ . Since the proton current available averaged about  $2 \mu\text{a}$ , the length of each bombardment was about 66 seconds.

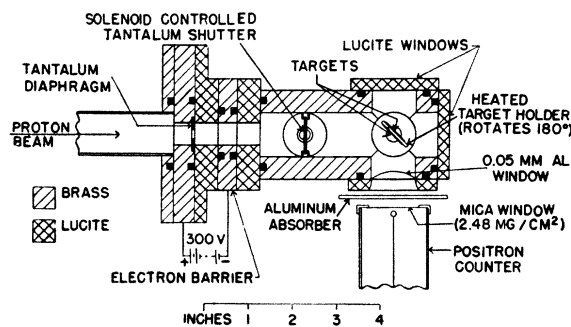


FIG. 5. Horizontal cross section of the positron counting arrangement.

A second circuit was constructed using relays and a clock to provide various timing and switching functions which were needed. This timing circuit operated in response to the normalization circuit as follows:

1. When the start button on the normalization circuit was pressed, the timing circuit released the solenoidally operated shutter in the target chamber and allowed the proton beam to strike the target.

2. When the normalization circuit indicated the proper bombardment, the timing circuit caused the shutter to be raised, started the clock, and turned off the belt spray voltage on the electrostatic generator.

3. After a 15-second delay, during which time the generator voltage decayed to a value at which the x-ray output was negligible, the timing circuit switched on the positron counting circuit.

4. At the end of a pre-set counting time, usually two minutes, the positron counting circuit was turned off, and all relays were returned to their initial positions. Provision was made to time the bombardment, delay, and counting periods, with electric timers to check on the accuracy of the circuit.

Figure 5 shows a horizontal cross section of the target chamber. The use of the tantalum shutter allowed a beam to be established before the bombardment was started. A heated target holder was used which could be rotated through an angle of  $180^\circ$  by remote control so that either one of two targets could be bombarded. Data were taken first on one target and then on the other according to the following sequence of operations: (1) establish beam, (2) bombardment, (3) delay time, (4) count positrons. At the start of counting on one target, the  $F^{17}$  produced in that target by the recent bombardment had only 15 sec to decay, while the  $F^{17}$  produced by a previous bombardment had about 7 half-lives to decay. Calculation shows that 85 percent of the activity to be measured remained at the start of counting, but only 0.8 percent of any previous activity was left. Thus, by the use of two targets, a waiting period between runs was avoided, and the resulting error due to old activity was less than the statistical fluctuation of the data.

A fraction of the positrons emitted from the target passed through the aluminum window of the target chamber and the aluminum absorber and were detected by a beta-ray counter of the end window type. The aluminum absorber was used between the target and the counter to reduce the counting rate from  $N^{13}$  and  $F^{18}$  positrons. Although the percentage of  $O^{18}$  in ordinary oxygen is small, the  $O^{18}(p,n)F^{18}$  reaction has a high cross section<sup>4,5</sup> above the 2.59-Mev threshold,<sup>14</sup> and the  $F^{18}$  activity can be greater than the  $F^{17}$  activity when an oxide target is bombarded with protons.  $N^{13}$  can be formed by the capture of protons by carbon on the target. A total absorber thickness of  $224 \text{ mg/cm}^2$  was used when data were being taken with the thick targets

<sup>14</sup> Richards, Smith, and Browne, Phys. Rev. **80**, 524 (1950).

and 258 mg/cm<sup>2</sup> when data were being taken with the thin targets. F<sup>18</sup> has a positron end point of  $635 \pm 15$  keV,<sup>15</sup> which is low enough so that all of the positrons from F<sup>18</sup> were stopped in the absorber. N<sup>13</sup> has a positron end point of  $1.202 \pm 0.005$  MeV,<sup>16</sup> which is so high in comparison with the  $1.72 \pm 0.03$ -MeV positron end point<sup>17</sup> of F<sup>17</sup> that it was not practical to use an absorber sufficiently thick to absorb all of the positrons from N<sup>13</sup>. Some experimental checks showed that no significant background of N<sup>13</sup> positrons was present, however. Since no resonances have been observed in the scattering of protons from carbon between 1.7 and 4.1 MeV,<sup>18</sup> there are probably no rapid fluctuations in the capture cross section over this energy region, and any background contributed by the presence of carbon should be fairly constant.

In order to determine background counting rates, approximately one out of every four runs was made using an aluminum absorber thickness of 4 mm. This absorber stopped all of the positrons from F<sup>17</sup>, but had little effect on the annihilation and x-radiation which formed most of the background. From the data thus obtained a background curve was plotted for each target. When thick oxide targets were used, the background amounted to about 10 percent of the total number of counts.

### Results

The entire energy range studied was covered twice, once with a pair of thick oxide targets, and once with a thinner pair. For each target of each pair the data were corrected for background and plotted separately. Within the experimental error, the data obtained from the two thin targets gave the same curve. One of the thick oxide targets contained about 50 percent more oxygen than the other, and the data obtained with one of these targets was multiplied by a normalization factor so that the two thick target yield curves would be nearly coincident.

Figure 6 shows the results of the capture cross section measurements. Data from both targets of the pair are included on both the curve representing the thick target data and the thin target data. The statistical uncertainty in the data is given approximately by the diameter of the circles which represent the data points.

The peculiar shapes of the step in the thick target data and the resonance peak in the thin target data near 3.47 MeV are largely due to the characteristics of the targets which were used. All data were taken with targets of tantalum oxidized by electrolysis in distilled water. Under the bombardment of a 2- $\mu$ a proton beam, the tantalum sometimes came to a dull red heat. Some

<sup>15</sup> Blaser, Boehm, and Marmier, Phys. Rev. **75**, 1953 (1949).

<sup>16</sup> Hornyak, Dougherty, and Lauritsen, Phys. Rev. **74**, 1727 (1948).

<sup>17</sup> V. Perez-Mendez and P. Lindenfeld, Phys. Rev. **80**, 1097 (1950).

<sup>18</sup> G. Goldhaber and R. M. Williamson, Phys. Rev. **82**, 495 (1951).

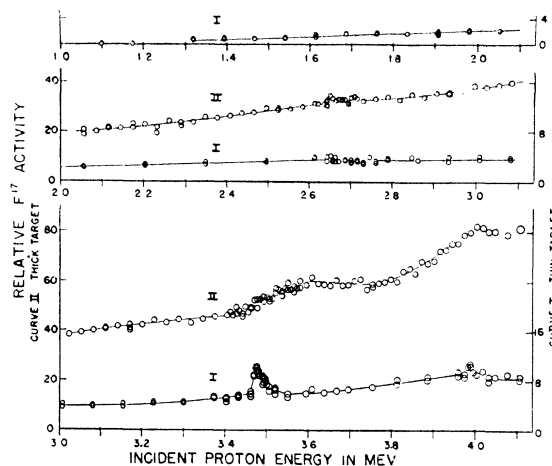


FIG. 6. Relative F<sup>17</sup> activity produced by the bombardment of oxide targets with protons.

of the oxygen which was originally on the surface of the target in the form of Ta<sub>2</sub>O<sub>5</sub> may have diffused into the target during bombardment, giving the distribution of oxygen in the tantalum target shown by the data. A thinner oxide target and better energy resolution of the proton beam were used to take the data of Fig. 7. Here again the observed shape of the resonance was determined by the characteristics of the target and the energy spread of the proton beam. The position of the narrow capture resonance was found to agree within the experimental error with the position of the 3.47-MeV resonance observed in the scattering experiment.

Other features of the variation of the capture cross section with energy which must be examined and correlated with the scattering data are: (1) the fact that within the experimental error the effect of the 2.66-MeV resonance on the capture cross section was not detectable, (2) the almost linear increase in the capture cross section above 3.75 MeV until a maximum is reached near 3.99 MeV. DuBridge, Barnes, Buck, and Strain<sup>5</sup> also found a rapidly increasing capture cross section as a function of energy near 3.9 MeV. The work

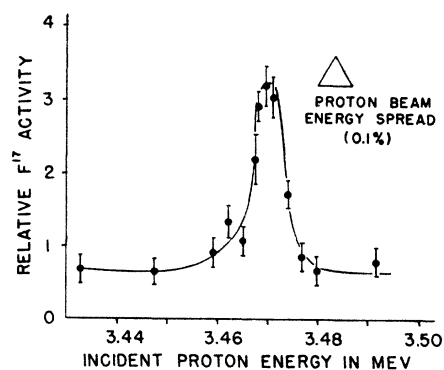


FIG. 7. F<sup>17</sup> activity produced by the bombardment of a thin oxide target with protons in the energy region near the 3.47-MeV resonance.

of these authors, combined with the present experiment, indicates that with the use of thick targets the more rapid rate of rise of the cross section above 3.75 Mev is more easily observed. A possible explanation of this effect is the presence of a broad capture resonance at 3.99 Mev. It has been assumed that this is the same resonance which causes the increase in the scattering cross section between 3.6 and 4.0 Mev.

#### IV. SUMMARY

The measurement of the elastic scattering and capture cross sections of oxygen for protons gives evidence for

resonances at proton energies of 2.66, 3.47, 3.99, and 4.39 Mev. The positions of the 2.66- and 3.47-Mev resonances are well determined, while the positions of the upper resonances are based on less substantial evidence. These four resonances correspond to energy levels in the compound nucleus,  $F^{17}$ , at 3.11, 3.88, 4.36, and 4.73 Mev.

The authors wish to thank Professor R. G. Herb, under whose supervision this project was carried out, for his advice and encouragement, and Dr. F. P. Mooring for assistance in taking some of the data.

### Assignment of Angular Momenta to the Energy Levels of $F^{17}$

R. A. LAUBENSTEIN\* AND M. J. W. LAUBENSTEIN\*

*University of Wisconsin, Madison, Wisconsin†*

(Received June 18, 1951)

An analysis of data on the elastic scattering and capture of protons by oxygen was made for the purpose of assigning angular momenta to certain energy levels in  $F^{17}$ . The elastic scattering data were analyzed using a graphic method wherein the phase and amplitude of the refracted partial waves are represented by vectors in the complex plane. As the proton energy is varied over a resonance, a circular locus is obtained for the vector which represents the component of a partial wave which excites the resonance.

Assignments of angular momenta to the energy levels of  $F^{17}$  have been made as follows: ground state,  $D_{\frac{3}{2}}$ ; 0.55 Mev,  $S_{\frac{3}{2}}$ ; 3.11 Mev,  $S_{\frac{3}{2}}$ ; 3.88 Mev,  $F_{\frac{3}{2}}$ ; 4.36 Mev,  $D_{\frac{3}{2}}$ ; and 4.73 Mev,  $P_{\frac{3}{2}}$ . The assignments of the 0.55-Mev, 3.11-Mev, and 3.88-Mev levels are reasonably certain, but the others are based on less substantial evidence. The reduced width of the 3.11-Mev  $S_{\frac{3}{2}}$  level was found to be about  $0.048 \times 10^{-13}$  Mev-cm, while the 0.55-Mev  $S_{\frac{3}{2}}$  level probably has a reduced width over 100 times as large.

The slowly rising capture cross section observed from 1.4 to 3.4 Mev is probably caused by the broad 0.55-Mev level.

A comparison of the levels in the mirror nuclei,  $O^{17}$  and  $F^{17}$ , shows a similar structure.

#### I. INTRODUCTION

THERE are a number of reasons to expect that experimental data obtained on the interaction of protons with  $O^{16}$  might be more easily interpreted than in the case of many other nuclei. For proton energies below about 5.6 Mev the only reactions which are energetically possible are elastic scattering and simple capture, with capture much less probable. Thus, complications introduced by several competing reactions are avoided. The binding energy of a proton added to an  $O^{16}$  nucleus is only 0.61 Mev, which is the lowest positive binding energy observed with any nucleus. Scattering of protons by  $O^{16}$ , therefore, gives information about the low-lying levels of  $F^{17}$ . Since the lower levels should have larger reduced widths and should be more widely spaced than the upper levels, the problems of experimentally resolving levels and plotting their shapes are less difficult.

Because the spin of  $O^{16}$  is zero, the scattering formulas are greatly simplified over the case of non-zero spin, and

the results of an elastic scattering experiment should be relatively easy to fit to these formulas.  $O^{16}$  contains 8 neutrons and 8 protons and can be considered as a closed shell in both neutrons and protons.<sup>1,2</sup> If this shell model of the nucleus is correct, the compound nucleus,  $F^{17}$ , formed under bombardment of  $O^{16}$  by protons, will consist of one proton outside a closed shell. The level structure of  $F^{17}$  is of theoretical interest because of the possibility of applying this simple nuclear model. Also,  $O^{17}$ , the mirror nucleus of  $F^{17}$ , has been rather extensively investigated; and it is of interest to compare the levels of these two nuclei.

The results of the previous paper on the elastic scattering and capture of protons by oxygen<sup>3</sup> are far from being sufficiently extensive, so that a detailed theoretical analysis can be made. However, it is interesting to attempt to fit these data to existing formulas, especially in view of the fact that no reaction yield involving a nucleus more complicated than lithium

<sup>1</sup> M. G. Mayer, Phys. Rev. **78**, 16 (1950).

<sup>2</sup> E. Feenberg and K. C. Hammack, Phys. Rev. **75**, 1877 (1949).

<sup>3</sup> Laubenstein, Laubenstein, Koester, and Mobley, Phys. Rev. **84** 12 (1951).

\* Now at North American Aviation, Inc., Downey, California.  
† Supported by the Wisconsin Alumni Research Foundation and the AEC.